

# Introduction to spherical field theory

Dean Lee<sup>1</sup>

Harvard University  
Cambridge, MA 02138

Spherical field theory is a new non-perturbative method for studying quantum field theories. It uses the spherical partial wave expansion to reduce a general  $d$ -dimensional Euclidean field theory into a set of coupled one-dimensional systems. The coupled one-dimensional systems are then converted to partial differential equations and solved numerically. We demonstrate the methods of spherical field theory by analyzing Euclidean  $\phi^4$  theory in two dimensions. [PACS numbers: 11.10.Kk, 11.15Tk, 11.30Qc]

## 1 Overview

We present a new non-perturbative method for studying quantum field theories. We describe a general procedure for converting problems in quantum field theory into initial-value problems described by partial differential equations. Our derivation of the method starts with the functional integral for a  $d$ -dimensional Euclidean field theory. Making use of spherical  $O(d)$ -symmetry, we decompose the fields as a linear combination of spherical partial waves. Re-interpreting the radial part of each partial wave as a distinct field in a new one-dimensional field theory, we rewrite the functional integral as a time-dependent Schrödinger equation, where the radial distance in the original theory serves as the time parameter. Although the resulting Schrödinger equation contains an infinite set of interacting partial waves, we find that high spin partial waves decouple if the original field theory is renormalized to remove ultraviolet divergences. Neglecting higher spin partial waves and estimating the corresponding error, we solve the remaining partial differential equation using standard methods.

---

<sup>1</sup>Supported by the National Science Foundation under Grant #PHY-9218167 and the Fannie and John Hertz Foundation.

The organization of this paper is as follows. We begin with a short discussion of one-dimensional systems and the connection between spherical field theory and coupled one-dimensional systems. Next we illustrate the method by analyzing normal-ordered Euclidean  $\phi^4$  theory in two dimensions. We derive the spherical Feynman rules for this theory, compute the two-loop self-energy, and compare the result with standard perturbation theory. We then consider non-perturbative values of the coupling constant and evaluate the self-energy numerically using finite-difference methods and diffusion Monte Carlo. Since our paper is intended as an introduction to the methods of spherical field theory rather than a detailed analysis of Euclidean  $\phi^4$  theory, we have not engaged in extensive numerical computations for our analysis here. Nevertheless, our rather modest calculations show clear evidence of spontaneously broken  $\phi \rightarrow -\phi$  reflection symmetry at the critical coupling value

$$\frac{\lambda}{4!(2\pi)\mu^2} \simeq 0.4, \quad (1)$$

where  $\mu$  is the bare mass and  $\lambda$  is defined by the quartic coupling  $\frac{\lambda}{4!}\phi^4$ . Our value of the critical coupling is in close agreement with the results of a recent lattice study [1]. The methods we present in this paper are easily generalized to any  $d$ -dimensional Euclidean field theory involving any number of scalar fields. The extension to fermionic and gauge systems is the subject of current work.

## 2 Spherical fields

We start with the Feynman-Kac formula, which connects the Schrödinger and path integral representations of (Euclideanized) quantum mechanics,

$$\begin{aligned} & \langle x_F | T \exp \left[ - \int_{t_I}^{t_F} dt H_{\mathcal{J}} \right] | x_I \rangle \\ & \propto \int_{\substack{\phi(t_I)=x_I \\ \phi(t_F)=x_F}} \mathcal{D}\phi \exp \left\{ - \int_{t_I}^{t_F} dt \left[ \frac{1}{2} \left( \frac{\partial \phi}{\partial t} \right)^2 + V(\phi) - \mathcal{J}\phi \right] \right\}, \end{aligned} \quad (2)$$

where

$$\begin{aligned} H_{\mathcal{J}}(t) &= -\frac{1}{2} \frac{d^2}{dq^2} + V(q) - \mathcal{J}q \\ &= H_0 - \mathcal{J}q \end{aligned} \quad (3)$$

and  $|x_I\rangle, |x_F\rangle$  are position eigenstates centered at  $x_I, x_F$ . The generating functional  $Z[\mathcal{J}]$  is proportional to the ground state persistence amplitude,

$$Z[\mathcal{J}] \propto \langle 0 | T \exp \left[ - \int_{-\infty}^{\infty} dt H_{\mathcal{J}} \right] | 0 \rangle, \quad (4)$$

where  $|0\rangle$  is the ground state of  $H_0$ . For  $t_1 > t_2$ ,

$$\left. \frac{1}{Z[0]} \frac{\delta^2 Z[\mathcal{J}]}{\delta \mathcal{J}(t_1) \delta \mathcal{J}(t_2)} \right|_{\mathcal{J}=0} = \frac{\langle 0 | T \exp \left[ - \int_{t_1}^{\infty} dt H_0 \right] q T \exp \left[ - \int_{t_2}^{t_1} dt H_0 \right] q T \exp \left[ - \int_{-\infty}^{t_2} dt H_0 \right] | 0 \rangle}{\langle 0 | T \exp \left[ - \int_{-\infty}^{\infty} dt H_0 \right] | 0 \rangle}. \quad (5)$$

The Feynman-Kac formula can be generalized to include more general time-dependent interactions,

$$\begin{aligned} & \langle x_F | T \exp \left[ - \int_{t_I}^{t_F} dt H(t) \right] | x_I \rangle \\ \propto & \int_{\substack{\phi(t_I)=x_I \\ \phi(t_F)=x_F}} \mathcal{D}\phi \exp \left\{ - \int_{t_I}^{t_F} dt \left[ \frac{1}{2a(t)} \left( \frac{\partial \phi}{\partial t} \right)^2 + V(\phi, t) \right] \right\}, \end{aligned} \quad (6)$$

where

$$H(t) = -\frac{a(t)}{2} \frac{d^2}{dq^2} + V(q, t). \quad (7)$$

The central idea of spherical field theory is to treat a general  $d$ -dimensional field theory as a set of coupled one-dimensional systems. To demonstrate, we consider Euclidean  $\phi^4$  theory in two dimensions,

$$Z[\mathcal{J}] = \int \mathcal{D}\phi \exp \left\{ - \int d^2x \left[ \frac{1}{2} \sum_i (\partial_i \phi)^2 + \frac{\mu^2}{2} \phi^2 + \frac{\lambda}{4!} \phi^4 - \mathcal{J}\phi \right] \right\}. \quad (8)$$

Decomposing  $\phi$  and  $\mathcal{J}$  into partial waves, we have

$$\phi(t \cos \theta, t \sin \theta) = \sqrt{\frac{1}{2\pi}} \sum_{n=0, \pm 1, \dots} \phi_n(t) e^{in\theta}, \quad (9)$$

$$\mathcal{J}(t \cos \theta, t \sin \theta) = \sqrt{\frac{1}{2\pi}} \sum_{n=0, \pm 1, \dots} \mathcal{J}_n(t) e^{in\theta}. \quad (10)$$

The decomposition of  $\phi$  into partial waves is a linear invertible transformation. The Jacobian of the transformation (tempered with suitable ultraviolet and infrared regulation) is,

$$\det \left[ \frac{\delta \phi(t' \cos \theta, t' \sin \theta)}{\delta \phi_n(t)} \right] = \det \left[ \sqrt{\frac{1}{2\pi}} \delta(t - t') e^{in\theta} \right]. \quad (11)$$

This Jacobian is independent of  $\phi_n(t)$ , and we change integration variables to write  $Z[\mathcal{J}]$  as

$$b \int \prod_{n=0,\pm 1,\dots} \mathcal{D}\phi_n \exp \left\{ - \int_0^\infty dt \left[ \sum_{n=0,\pm 1,\dots} \frac{t}{2} \frac{\partial \phi_{-n}}{\partial t} \frac{\partial \phi_n}{\partial t} + \frac{\mu^2 t^2 + n^2}{2t} \phi_{-n} \phi_n - t \mathcal{J}_{-n} \phi_n \right. \right. \\ \left. \left. + \frac{\lambda t}{4! 2\pi} \sum_{\substack{n_1, n_2, n_3 \\ =0,\pm 1,\dots}} \phi_{n_1} \phi_{n_2} \phi_{n_3} \phi_{-n_1 - n_2 - n_3} \right] \right\}, \quad (12)$$

where  $b$  is an overall constant whose value is irrelevant for the purposes of our discussion. From (6) and (7), this functional integral corresponds with the Schrödinger time evolution generator

$$H_{\mathcal{J}} = \sum_{n=0,\pm 1,\dots} -\frac{1}{2t} \frac{\partial}{\partial q_{-n}} \frac{\partial}{\partial q_n} + \frac{\mu^2 t^2 + n^2}{2t} q_{-n} q_n - t \mathcal{J}_{-n} q_n \\ + \frac{\lambda t}{4! 2\pi} \sum_{\substack{n_1, n_2, n_3 \\ =0,\pm 1,\dots}} q_{n_1} q_{n_2} q_{n_3} q_{-n_1 - n_2 - n_3}. \quad (13)$$

In order to define  $Z[\mathcal{J}]$  in the Schrödinger language, we first restrict the  $t$ -integral in (12) to a finite interval,  $t_I \leq t \leq t_F$ . We then have

$$Z_{[t_I, t_F]}[\mathcal{J}] \propto \int \prod_{n=0,\pm 1,\dots} dx_n dx'_n \langle \{x'_n\}_{n=0,\pm 1,\dots} | T \exp \left[ - \int_{t_I}^{t_F} dt H_{\mathcal{J}}(t) \right] | \{x_n\}_{n=0,\pm 1,\dots} \rangle, \quad (14)$$

where

$$q_i | \{x_n\}_{n=0,\pm 1,\dots} \rangle = x_i | \{x_n\}_{n=0,\pm 1,\dots} \rangle. \quad (15)$$

We recover  $Z[\mathcal{J}]$  by taking the limits  $t_I \rightarrow 0$ ,  $t_F \rightarrow \infty$ . The details of the quantum state at the boundary  $t_F$  is rather unimportant since only the ground state projection survives as  $t_F \rightarrow \infty$ , similar to what happens in (4). In contrast, the  $q_0$  dependence of the quantum state at  $t_I = 0$  is significant.<sup>1</sup> The proper initial state is

$$|a\rangle \equiv \int \prod_{n=0,\pm 1,\dots} dx_n | \{x_n\}_{n=0,\pm 1,\dots} \rangle, \quad (16)$$

a state whose wavefunction is constant in  $q$ -space.

---

<sup>1</sup>For  $n \neq 0$  the  $q_n$  dependence is again unimportant and depends only on the ground state projection.

### 3 Correlators

The generating functional, written as a power series, is

$$\frac{Z[\mathcal{J}]}{Z[0]} = 1 + \frac{1}{2} \int \frac{d^2\vec{p}d^2\vec{x}d^2\vec{y}}{(2\pi)^2} e^{-i\vec{p}\cdot\vec{x}} e^{i\vec{p}\cdot\vec{y}} \mathcal{J}(\vec{x}) \mathcal{J}(\vec{y}) f(\vec{p}^2) + \dots, \quad (17)$$

where  $f(\vec{k}^2)$  is the  $\phi$  propagator,

$$f(\vec{k}^2) = \int d^2\vec{x} e^{i\vec{k}\cdot\vec{x}} \langle 0 | \phi(\vec{x}) \phi(0) | 0 \rangle. \quad (18)$$

As a result of angular momentum conservation, the term quadratic in  $\mathcal{J}$  can be decomposed as a sum over terms proportional to  $\mathcal{J}_{-n}\mathcal{J}_n$ ,

$$\frac{1}{2} \sum_{n=0,\pm 1,\dots} \int dk dt_x dt_y t_x t_y k \mathcal{J}_{-n}(t_x) \mathcal{J}_n(t_y) J_{|n|}(kt_x) J_{|n|}(kt_y) f(k^2), \quad (19)$$

where  $J_i$  is the  $i^{\text{th}}$  order Bessel function of the first kind. The two-point correlator for the  $n$ -th partial wave is

$$\langle 0 | \phi_{-n}(t_1) \phi_n(t_2) | 0 \rangle = \frac{1}{Z[0]} \frac{\delta^2 Z[\mathcal{J}]}{t_1 \delta \mathcal{J}_n(t_1) t_2 \delta \mathcal{J}_{-n}(t_2)} \Big|_{\mathcal{J}=0} = \int dk k J_{|n|}(kt_1) J_{|n|}(kt_2) f(k^2). \quad (20)$$

We will use this result in the next section when discussing perturbative spherical field theory. For the special case  $n = 0$  and  $t_2 = 0$  we have

$$\begin{aligned} \langle 0 | \phi_0(t_1) \phi_0(0) | 0 \rangle &= \int dk k J_0(kt_1) f(k^2) = \int \frac{d^2\vec{p}}{2\pi} e^{-i\vec{p}\cdot\vec{x}} f(\vec{p}^2) \\ &= 2\pi \langle 0 | \phi(\vec{r}) \phi(0) | 0 \rangle, \end{aligned} \quad (21)$$

when  $|\vec{r}| = t_1$ . The two-point  $\phi$  correlator is proportional to the two-point  $\phi_0$  correlator with one  $\phi_0$  centered at the origin. We can compute the two-point  $\phi_0$  correlator using the Schrödinger formalism,

$$\langle 0 | \phi_0(t_1) \phi_0(0) | 0 \rangle = \frac{\langle a | T \exp \left[ - \int_{t_1}^{\infty} dt H_0 \right] q_0 T \exp \left[ - \int_0^{t_1} dt H_0 \right] q_0 | a \rangle}{\langle a | T \exp \left[ - \int_0^{\infty} dt H_0 \right] | a \rangle}. \quad (22)$$

More general correlation functions can be evaluated by partial wave expansion. For example the four-point  $\phi$  correlator is given by

$$\langle 0 | \phi(\vec{r}_1) \phi(\vec{r}_2) \phi(\vec{r}_3) \phi(0) | 0 \rangle = \sum_{\substack{n_1, n_2, n_3 \\ =0, \pm 1, \dots}} \frac{e^{i(n_1\theta_1 + n_2\theta_2 + n_3\theta_3)}}{(2\pi)^2} \langle 0 | \phi_{n_1}(t_1) \phi_{n_2}(t_2) \phi_{n_3}(t_3) \phi_0(0) | 0 \rangle \quad (23)$$

where

$$\vec{r}_i = (t_i \cos \theta_i, t_i \sin \theta_i), \quad i = 1, 2, 3. \quad (24)$$

In the Schrödinger formalism, we can rewrite

$$\langle 0 | \phi_{n_1}(t_1) \phi_{n_2}(t_2) \phi_{n_3}(t_3) \phi_0(0) | 0 \rangle \quad (25)$$

as (for  $t_1 \geq t_2 \geq t_3$ ),

$$\frac{\langle a | T \exp \left[ - \int_{t_1}^{\infty} dt H_0 \right] q_{n_1} T \exp \left[ - \int_{t_2}^{t_1} dt H_0 \right] q_{n_2} T \exp \left[ - \int_{t_3}^{t_2} dt H_0 \right] q_{n_3} T \exp \left[ - \int_0^{t_3} dt H_0 \right] q_0 | a \rangle}{\langle a | T \exp \left[ - \int_0^{\infty} dt H_0 \right] | a \rangle}. \quad (26)$$

## 4 Perturbative spherical field theory

For free field theory we have  $f(\vec{k}^2) = \frac{1}{k^2 + \mu^2}$ . From (20),

$$\langle 0 | \phi_{-n}(t_1) \phi_n(t_2) | 0 \rangle = \theta(t_1 - t_2) K_{|n|}(\mu t_1) I_{|n|}(\mu t_2) + \theta(t_2 - t_1) K_{|n|}(\mu t_2) I_{|n|}(\mu t_1), \quad (27)$$

where  $I_i$  and  $K_i$  are the  $i^{\text{th}}$  order modified Bessel functions of the first and second kind respectively. In particular, we find

$$\langle 0 | \phi_0(t) \phi_0(0) | 0 \rangle = K_0(\mu t). \quad (28)$$

We can use (27) to generate the spherical version of Feynman diagrams. As an example, the two-loop process shown in Figure 1 gives us

$$\int dt_1 dt_2 \frac{\lambda^2 t_1 t_2}{(2\pi)^2} \left[ \begin{array}{c} \theta(t - t_1) K_0(\mu t) I_0(\mu t_1) \\ + \theta(t_1 - t) K_0(\mu t_1) I_0(\mu t) \end{array} \right] \left[ \begin{array}{c} \theta(t_1 - t_2) K_{1,2,3}(\mu t_1) I_{1,2,3}(\mu t_2) \\ + \theta(t_2 - t_1) K_{1,2,3}(\mu t_2) I_{1,2,3}(\mu t_1) \end{array} \right] K_0(\mu t_2), \quad (29)$$

where

$$\begin{aligned} I_{1,2,3}(x) &= I_1(x) I_2(x) I_3(x), \\ K_{1,2,3}(x) &= K_1(x) K_2(x) K_3(x). \end{aligned} \quad (30)$$

This diagram contributes to the two-point  $\phi_0$  correlator at order  $\lambda^2$ . Let  $\Delta_{2, J_{\max}}(t)$  be the sum of all such  $O(\lambda^2)$  diagrams for the  $\phi_0$  correlator, with the restriction that each internal line correspond with some  $\phi_n$  such that

$|n| \leq J_{\max}$ . In view of relation (21) we expect that as  $J_{\max} \rightarrow \infty$  we should recover the regular two-loop perturbative result,

$$\lim_{J_{\max} \rightarrow \infty} \frac{1}{2\pi} \int dt d\theta t e^{itk \cos \theta} \Delta_{2, J_{\max}}(t) = \frac{\lambda^2}{96\pi^2(k^2 + \mu^2)^2} \int_0^1 \int_0^{1-\alpha_1} \frac{d\alpha_2 d\alpha_1 \delta(\alpha_1 + \alpha_2 + \alpha_3 - 1)}{\alpha_1 \alpha_2 \alpha_3 k^2 + (\alpha_1 \alpha_2 + \alpha_2 \alpha_3 + \alpha_3 \alpha_1) \mu^2}. \quad (31)$$

In Figure 2 we have plotted

$$s_{J_{\max}}(k^2) \equiv \frac{48\pi(k^2 + \mu^2)^2}{\lambda^2} \int dt d\theta t e^{itk \cos \theta} \Delta_{2, J_{\max}}(t), \quad J_{\max} = 0, 1, 2, 3, \quad (32)$$

and

$$s_{\infty}(k^2) \equiv \int_0^1 \int_0^{1-\alpha_1} \frac{d\alpha_2 d\alpha_1}{\alpha_1 \alpha_2 \alpha_3 k^2 + (\alpha_1 \alpha_2 + \alpha_2 \alpha_3 + \alpha_3 \alpha_1) \mu^2}, \quad (33)$$

in units where  $\mu = 1$ . It appears that  $s_{J_{\max}}(k^2)$  does in fact converge towards  $s_{\infty}(k^2)$ . We discuss this and related issues in the next section.

## 5 High spin decoupling

Partial waves with high spin correspond with high tangential momentum modes. We can see this explicitly in the coefficient of  $\phi_{-n}\phi_n$  in (12),

$$\frac{\mu^2 t^2 + n^2}{2t}, \quad (34)$$

where the  $n^2$  dependence is generated by the centrifugal part of the kinetic term

$$\frac{1}{2} \sum_i (\partial_i \phi)^2. \quad (35)$$

Therefore if our field theory is renormalized to remove ultraviolet divergences, the contribution of high spin partial waves will decouple in the same manner as other high momentum effects such as dependence on an explicit cutoff mass scale. The error in neglected partial waves with spin larger than some value  $J_{\max}$  is roughly equivalent to the error in using a cutoff mass  $\Lambda_{\text{eff}}$  where

$$\Lambda_{\text{eff}}^2 \sim \frac{J_{\max}^2}{t^2}, \quad (36)$$

and  $t$  is the characteristic radius for the process being studied.

In two-dimensional  $\phi^4$  theory, renormalization can be done simply by normal ordering the interaction. In the context of spherical field, normal ordering corresponds with explicitly subtracting the contribution of diagrams

of the type shown in Figure 3. The amplitude for this diagram is proportional to

$$\lambda t K_{|n|}(\mu t) I_{|n|}(\mu t). \quad (37)$$

In the Schrödinger language this corresponds with a counterterm proportional to

$$\lambda t K_{|n|}(\mu t) I_{|n|}(\mu t) q_{-i} q_i. \quad (38)$$

Let us now return to the two-loop perturbative calculation. In presence of an explicit cutoff mass  $\Lambda_{\text{eff}}$ , the  $\Lambda_{\text{eff}}$ -regulated calculation for the two-loop result  $s_\infty(k^2)$  includes a correction of size  $O(\Lambda_{\text{eff}}^{-2})$ . From relation (36), we expect

$$s_\infty(k^2) - s_{J_{\text{max}}}(k^2) \sim O(J_{\text{max}}^{-2}). \quad (39)$$

## 6 Non-perturbative self-energy

Let us define  $c = \frac{\lambda}{4!(2\pi)}$  and  $\Delta(t)$  to be the difference between the two-point  $\phi_0$  correlator for general  $c$  and  $c = 0$ ,

$$\Delta(t) = \langle 0 | \phi_0(t) \phi_0(0) | 0 \rangle_c - \langle 0 | \phi_0(t) \phi_0(0) | 0 \rangle_{c=0}. \quad (40)$$

We can compute  $\Delta(t)$  using (13) and (22) along with normal-ordering counterterms described in the previous section. For  $c = 0.20$  we have computed  $\Delta(t)$  for  $J_{\text{max}} = 0$  and  $J_{\text{max}} = 1$ . For  $J_{\text{max}} = 0$  the Schrödinger time evolution generator is

$$-\frac{1}{2t} \frac{\partial^2}{\partial q_0^2} + \frac{\mu^2 t}{2} q_0^2 + ct q_0^4 - 6ct K_0(\mu t) I_0(\mu t) q_0^2. \quad (41)$$

For  $J_{\text{max}} = 1$  the time evolution generator is

$$\begin{aligned} & -\frac{1}{2t} \left[ \frac{\partial^2}{\partial q_0^2} + \frac{\partial^2}{\partial q_{s1}^2} + \frac{\partial^2}{\partial q_{a1}^2} \right] + \frac{\mu^2 t}{2} q_0^2 + \frac{\mu^2 t^2 + 1}{2t} (q_{s1}^2 + q_{a1}^2) \\ & + ct \left[ q_0^4 + \frac{3}{2} (q_{s1}^2 + q_{a1}^2)^2 + 6q_0^2 (q_{s1}^2 + q_{a1}^2) \right] \\ & - 6ct [K_0(\mu t) I_0(\mu t) + 2K_1(\mu t) I_1(\mu t)] [q_0^2 + q_{s1}^2 + q_{a1}^2], \end{aligned} \quad (42)$$

where

$$q_{s1} = \frac{q_1 + q_{-1}}{\sqrt{2}}, \quad q_{a1} = \frac{q_1 - q_{-1}}{i\sqrt{2}}. \quad (43)$$

For each value of  $J_{\text{max}}$  we did the computation two ways, once using the method of finite differences and once using diffusion Monte Carlo. The results

are shown in Figure 4, where we have used the abbreviations fd for finite difference method and mc for Monte Carlo. This plot should be regarded as a measure of the accuracy of the Monte Carlo algorithm. The error of the finite difference algorithm is likely negligible as we were able to reproduce the two-point  $\phi_0$  correlator for free field theory to an accuracy of 0.1%.

Let  $\Pi(k^2)$  denote the  $\phi$  self-energy, defined such that the full  $\phi$  propagator is

$$f(k^2) = \frac{1}{k^2 + \mu^2 + \Pi(k^2)}. \quad (44)$$

We have calculated  $-\Pi(k^2)$  for  $c = 0.05, 0.10, \dots, 0.40$  and  $J_{\max} = 2$ . For  $J_{\max} = 2$  the time evolution generator is

$$\begin{aligned} & -\frac{1}{2t} \left[ \frac{\partial^2}{\partial q_0^2} + \frac{\partial^2}{\partial q_{s1}^2} + \frac{\partial^2}{\partial q_{a1}^2} + \frac{\partial^2}{\partial q_{s2}^2} + \frac{\partial^2}{\partial q_{a2}^2} \right] \\ & + \frac{\mu^2 t}{2} q_0^2 + \frac{\mu^2 t^2 + 1}{2t} (q_{s1}^2 + q_{a1}^2) + \frac{\mu^2 t^2 + 4}{2t} (q_{s2}^2 + q_{a2}^2) \\ & + ct \left[ \begin{aligned} & q_0^4 + \frac{3}{2} (q_{s1}^2 + q_{a1}^2)^2 + \frac{3}{2} (q_{s2}^2 + q_{a2}^2)^2 + 6q_0^2 (q_{s1}^2 + q_{a1}^2 + q_{s2}^2 + q_{a2}^2) \\ & + 6\sqrt{2} q_0 (q_{s1}^2 q_{s2} - q_{a1}^2 q_{s2} + 2q_{a1} q_{s1} q_{a2}) + 6(q_{s1}^2 + q_{a1}^2)(q_{s2}^2 + q_{a2}^2) \end{aligned} \right] \\ & - 6ct [K_0(\mu t)I_0(\mu t) + 2K_1(\mu t)I_1(\mu t) + 2K_2(\mu t)I_2(\mu t)] \cdot \left[ \begin{aligned} & q_0^2 + q_{s1}^2 + q_{a1}^2 \\ & + q_{s2}^2 + q_{a2}^2 \end{aligned} \right] \end{aligned} \quad (45)$$

where

$$q_{s2} = \frac{q_2 + q_{-2}}{\sqrt{2}}, \quad q_{a2} = \frac{q_2 - q_{-2}}{i\sqrt{2}}. \quad (46)$$

Our results were calculated using diffusion Monte Carlo and are shown in Figure 5. The physical squared-mass  $\mu_{\text{phys}}^2$  can be found by extrapolating  $-\Pi(k^2)$  to its intersection point with the line  $k^2 + 1$  (in units where the bare mass  $\mu = 1$ ),

$$-\Pi(-\mu_{\text{phys}}^2) = -\mu_{\text{phys}}^2 + 1. \quad (47)$$

One fact that is useful in performing this extrapolation is

$$-\frac{d\Pi}{dk^2} \Big|_{k^2 = -\mu_{\text{phys}}^2} \leq 0, \quad (48)$$

since the residue of the pole at  $-\mu_{\text{phys}}^2$  must be less than or equal to 1.<sup>2</sup> As Figure 5 shows (and also visible in the plots of  $s_{J_{\max}}(k^2)$  in Figure 2), the slope of  $-\Pi(k^2)$  appears to have the wrong sign at small values of  $k^2$ . The reason for this is that high spin partial waves cannot be neglected for  $t \sim O(J_{\max})$ ,

<sup>2</sup>This can be proved by spectral decomposition of the two-point  $\phi$  correlator.

or equivalently  $k^2 \sim O(J_{\max}^{-2})$ . It is therefore necessary to extrapolate  $-\Pi(k^2)$  from values of  $k^2$  where this breakdown does not occur.

Extrapolating  $-\Pi(k^2)$  through the small  $k^2$  region is somewhat difficult for  $J_{\max} = 2$ , and we could achieve greater accuracy by choosing a higher value for  $J_{\max}$ . But, as mentioned before, our main goal here is to introduce to the methods of spherical field theory. A more thorough and accurate calculation of this and other phenomena will be done in the future. For now the extrapolation method we choose is simply to extend the maximum value of  $-\Pi(k^2)$  to all  $k^2$  to the left of the maximum, as shown by the horizontal dashed lines in Figure 5. With this simple procedure we find the following values of  $\mu_{\text{phys}}^2$ .

$c$	$\mu_{\text{phys}}^2$	
0	1	
0.05	0.95	
0.10	0.8	
0.15	0.65	
0.20	0.5	(49)
0.25	0.35	
0.30	0.2	
0.35	0.1	
0.40	0.0	

For  $c$  near 0.4 the physical mass vanishes. As discussed in the literature, [2] and [3], this is associated with spontaneous breaking of  $\phi \rightarrow -\phi$  reflection symmetry. Despite using a small value for  $J_{\max}$  and a minimal amount of computer labor, we find that our value for the critical coupling is in agreement with a recent lattice calculation, [1], which found the critical coupling at  $c = 0.407$ .

## 7 Summary

Spherical field theory is a new approach to studying quantum field theory. It treats a general  $d$ -dimensional field theory as a system of coupled one-dimensional theories, which are then solved using partial differential equations. In this paper we introduced the methods of spherical field theory using the example of Euclidean  $\phi^4$  theory in two dimensions. We first derived the spherical Feynman rules, showed that high spin partial waves decouple, and

then, using a spin cutoff  $J_{\max} = 2$ , computed the  $\phi$  self-energy for non-perturbative values of the coupling. Our results show clear evidence of a phase transition near  $c = 0.4$ . The methods used here are easily generalized to any  $d$ -dimensional Euclidean field theory involving scalar fields. The extension to fermionic and gauge systems is currently being studied.

We expect spherical field theory to have many applications in the areas of particle theory and statistical physics. It offers an efficient and flexible way to calculate non-perturbative quantities in field theory. For simple systems (small  $J_{\max}$ ) either the method of finite differences or Monte Carlo simulation can be used. For larger systems only Monte Carlo methods are feasible, but here again we have several qualitatively different options. In our computation of the  $\phi$  self-energy we used diffusion Monte Carlo to model the time evolution equation. Another option, though, is to compute the one-dimensional path integral shown in (12) using standard lattice field methods. The ability to calculate quantities in several different ways is often useful in finding efficient algorithms and error-checking. In this regard we believe spherical field calculations should be useful in lattice field calculations and vice versa.

## Acknowledgements

The author wishes to thank George Brandenburg for use of computing facilities, Jong Lee for discussions on numerical methods, Sidney Coleman and Arthur Jaffe for discussions on  $\phi^4$  theory in two dimensions, and Howard Georgi for numerous conversations and guidance through all stages of this project.

## References

- [1] W. Loinaz and R.S. Willey, hep-lat/9712008 (1997).
- [2] J. Glimm and A. Jaffe, Phys. Rev. D10, 536 (1974).
- [3] J. Glimm, A.Jaffe, and T. Spencer, Comm. Math. Phys. 45, 203 (1975).

Figure 1. The two-loop self-energy diagram for  $\phi_0$ .

Figure 2. Plot of the two-loop self-energy, with normalization given in (32), for  $J_{\max} = 0, 1, 2, 3, \infty$ .

Figure 3. The only divergent diagram, which can be removed by normal ordering.

Figure 4. Plots for  $\Delta(t)$  as calculated by finite difference (fd) and Monte Carlo (mc) methods, with  $J_{\max} = 0, 1$  and  $c = 0.20$ .

Figure 5. Plots for  $-\Pi(k^2)$  with  $J_{\max} = 2$  and  $c = 0.05, 0.10, \dots, 0.40$ .

Figure 1

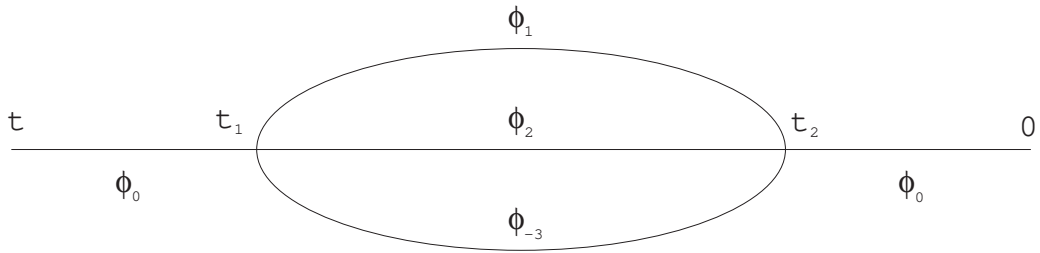


Figure 2

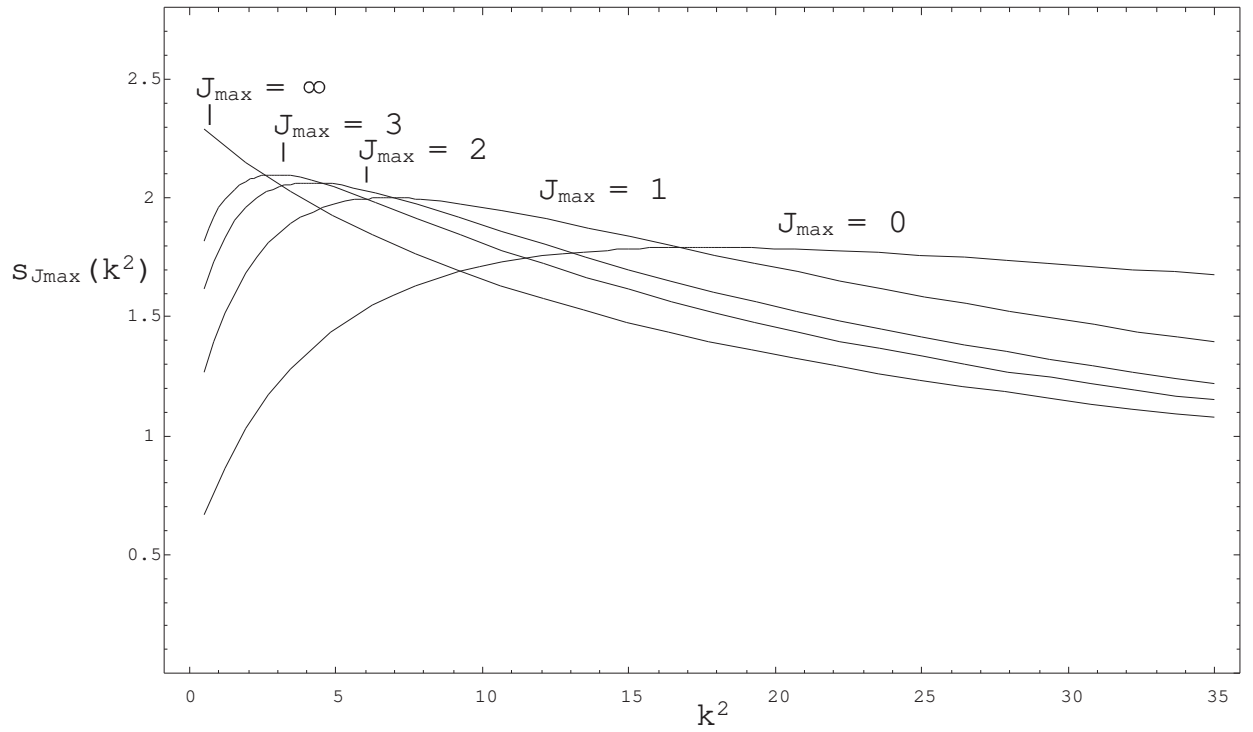


Figure 3

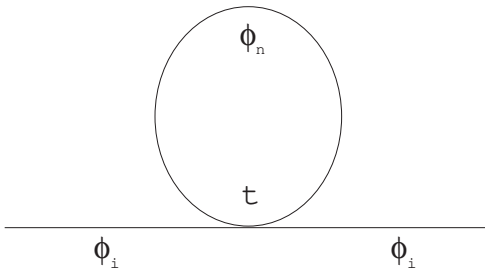


Figure 4

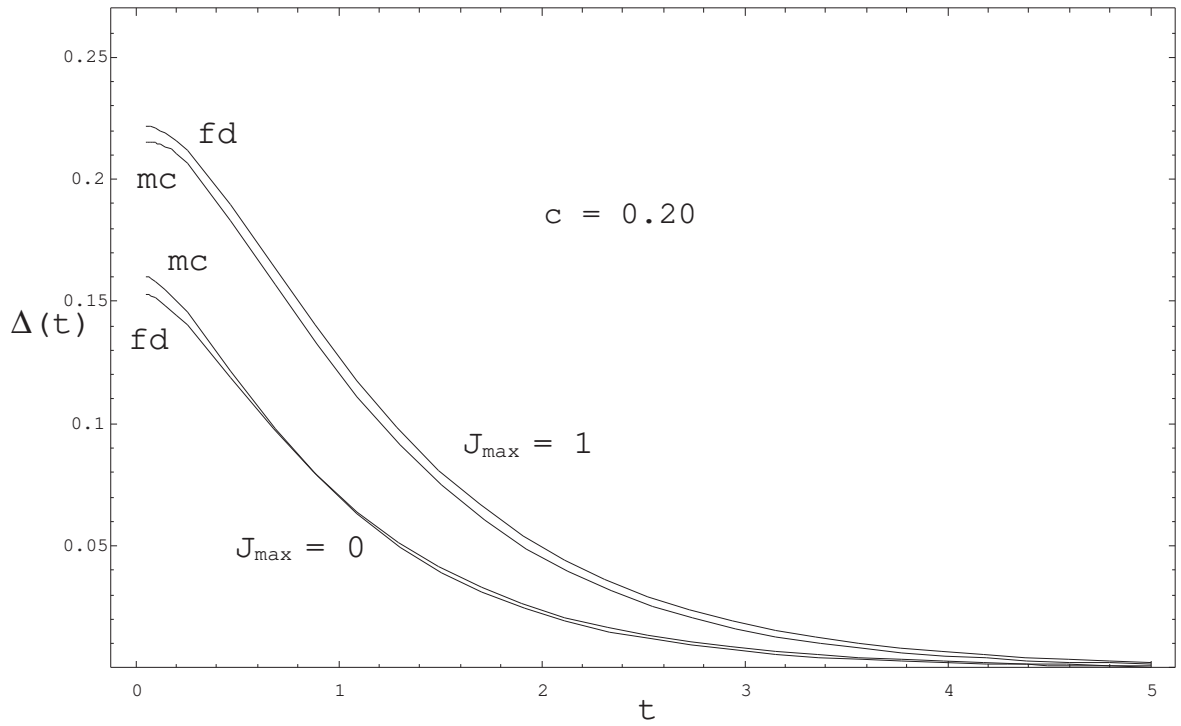


Figure 5

